Photoinduced Electron Transfer in "Two-Point" Bound Supramolecular Triads Composed of N,N-Dimethylaminophenyl-Fullerene-Pyridine Coordinated to Zinc Porphyrin

ARTICLE *in* THE JOURNAL OF PHYSICAL CHEMISTRY A · MAY 2003

Impact Factor: 2.69 · DOI: 10.1021/jp030363w

Photoinduced Electron Transfer in "Two-Point" Bound Supramolecular Triads Composed of *N,N*-Dimethylaminophenyl-Fullerene-Pyridine Coordinated to Zinc Porphyrin

Francis D'Souza,*,† Gollapalli R. Deviprasad,† Melvin E. Zandler,† Mohamed E. El-Khouly,‡ Mamoru Fujitsuka,‡ and Osamu Ito*,‡

Department of Chemistry, Wichita State University, 1845 Fairmount, Wichita, Kansas 67260-0051, and Institute of Multidisciplinary Research for Advanced Materials, Tohoku University, CREST, JST, Katahira, Sendai 980-8577, Japan

Received: March 24, 2003

Stable with defined distance and orientation, self-assembled supramolecular triads composed of *N,N*-dimethylaminophenylfullerene−pyridine bound to zinc porphyrins by a newly developed "two-point" binding strategy are reported. For this, zinc porphyrin was derivatized to bear "hydrogen-bonding" functionalities, carboxylic acid or amide groups, and C_{60} was functionalized to bear a ligating group, pyridine, and a second electron donor, *N,N*-dimethylaminophenyl group. The supramolecular triads formed by self-assembly of the zinc porphyrin and fullerene derivatives via the two-point binding method were characterized by spectroscopic and electrochemical techniques and were modeled by using ab initio computational methods. Evidence for axial coordination of the pyridine entity to the zinc metal center and H-bonding between the pyrrolidine ring nitrogen and the pendant carboxylic acid or amide groups was obtained. In the supramolecular triads, the second electron donor, *N,N*-dimethylaminophenyl, promotes efficient charge separation upon excitation of the zinc porphyrin to yield the radical ion pairs. The radical ion pairs thus generated undergo slow charge recombination to yield relatively long-lived (30−40 ns) charge-separated states.

Introduction

Photosynthetic reaction centers of green plants and bacteria consist of complex arrays of chromophores noncovalently attached to a protein scaffold, which fixes the cofactors in an appropriate orientation and spatial separation for efficient vectorial electron transfer.[1] The protein also provides an anisotropic medium to modulate the chemical properties of the cofactors and directs the electron-transfer pathways. Macrocyclic receptors designed to mimic the structural features of intermolecular interactions and thermodynamic parameters have given insight into the mechanism of the self-assembly process. Several covalently and noncovalently linked donor−acceptor entities with fixed distance and orientation have been designed and studied in this regard.[2] These studies have yielded reasonably good knowledge of the distance between the two groups, their relative spatial orientation, and the nature of the pathway linking the two components, which can act as a conduit for the energy or electron transfer. It has therefore been possible to relate the rate and efficiency of the interaction to the distance between the components, the conformation of the bridge, and the presence and absence of direct orbital overlap between the components.

Interestingly, although fullerenes[3] are now recognized to be better electron acceptors with regard to their redox potential,[4] reorganization energy,[5] and structure,[6] only a limited number of noncovalently linked model systems have been developed to address some of the fundamental questions with regard to distance and orientation and their effects on the rates of electron transfer.[2g,7,8] Among the different self-assembly approaches, fullerenes functionalized to bear metal-ligating groups[7] are attractive ones. The metal-ligating groups have been successfully utilized to bind the metal center of metallotetrapyrrole complexes. With the use of this approach, several self-assembled dyads and triads have been constructed and investigated. In one study, control over the distance and orientation was accomplished by an elegantly designed "two-point" binding approach involving covalent and coordinate bonds.[7f] In the present study, we have constructed supramolecular triads composed of 5-(*N,N*-dimethylaminophenyl)-2-(methylene-4′-pyridyl)fulleropyrrolidine (**1**) bound to functionalized zinc porphyrins. Here, a "one-point" binding approach involving axial coordination of the pyridine to the central metal ion and a "two-point" binding approach involving hydrogen-bonding groups in addition to the axial coordination of the pyridine to the central metal ion (Figure 1) have been developed. The pyrrolidine ring nitrogen forms a hydrogen bond with the appended carboxylic acid or the amide group of the porphyrin macrocycle thus enhancing the stability of the self-assembled complexes. In the studied triads, the zinc porphyrin acts as a primary electron donor, C_{60} acts as a primary electron acceptor, and the *N,N*-dimethylaminophenyl entity acts as a secondary electron donor. Introduction of *N,N*-dimethylaminophenyl demonstrates efficient charge separation followed by the generation of the relatively long-lived charge-separated states.

Experimental Section

Chemicals. Buckminsterfullerene, C_{60} (+99.95%), was from SES Research (Houston, TX). *o*-Dichlorobenzene in sure-seal bottle, sarcosine, pyrrole, and benzaldehyde derivatives were from Aldrich Chemicals (Milwaukee, WI). *d*-4-Pyridylalanine was from Pep Tech Corp (CA). Tetra-*n*-butylammonium perchlorate, $(TBA)ClO_4$, was from Fluka Chemicals. All chemicals were used as received.

5-(*N,N*-Dimethylaminophenyl)-2-(methylene-4′-pyridyl)fulleropyrrolidine (**1**) was synthesized by refluxing a mixture of

† Wichita State University.
‡ Tohoku University.

10.1021/jp030363w CCC: $25.00
Published on Web 05/20/2003

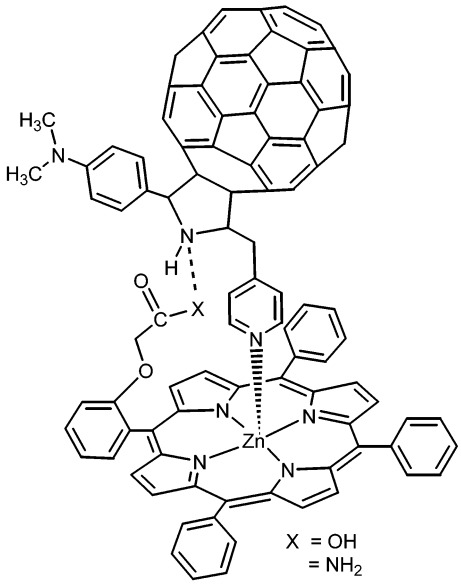

Figure 1. Structure of the "two-point" bound supramolecular triads investigated in the present study.

C_{60} (100 mg), 4-pyridylalanine (52 mg), and 4-(*N*,*N*-dimethylamino)benzaldehyde (80 mg) in toluene (100 mL) for 12 h according to a general procedure of fulleropyrrolidine synthesis developed by Prato and co-workers.[9] At the end, the solvent was removed and the crude product was purified over a silica gel column using ethyl acetate and toluene as eluent. ^{1}H NMR in $CS_2/CDCl_3$ (1:1 v/v), δ: 8.64, 7.72 (s (br), d, 2H, 2H, pyridine), 7.59, 6.61 (d, d, 2H, 2H, phenyl), 5.63, 5.00, 4.01, 3.50 (s, d, d, q, 1H, 1H, 1H, 1H, pyrrolidine and $-CH_2$), 2.94 (s, 6H, $-CH_3$). Electrospray ionization (ESI) mass in CH_2Cl_2: calcd. 973.0, found 972.8. The synthesis of 2-(4′-pyridyl)-fulleropyrrolidine is given elsewhere.[7g]

Free base 5-(2-phenoxyacetic acid)-10,15,20-triphenylporphyrin ($H_2P-COOH$) and 5-(2-phenoxyacetamide)-10,15,20-triphenylporphyrin ($H_2P-CONH_2$) were synthesized by reacting stoichiometric amounts of pyrrole, benzaldehyde, and the appropriate ortho-substituted benzaldehydes in propionic acid followed by column chromatography purification on either basic alumina or silica gel.[10] The ortho-substituted benzaldehydes, (2-formylphenoxy)acetic acid and (2-formylphenoxy)acetamide, were synthesized according to the literature procedure.[11] Zinc insertion was carried out according to the standard procedure[12] to obtain 5-(2-phenoxyacetic acid)-10,15,20-triphenylporphyrinatozinc (ZnP−COOH) and 5-(2-phenoxyacetamide)-10,15,-20-triphenylporphyrinatozinc ($ZnP-NH_2$). The molecular integrity of all of the synthesized free-base and zinc porphyrins was established from ESI mass and ^{1}H NMR studies. ^{1}H NMR in $CDCl_3$, δ ppm, $H_2P-COOH$: 8.92 (m, 8H, β-pyrrole), 8.18 (m, 6H, ortho phenyl), 7.71 (m, 9H, meta and para phenyl), 7.32−7.16 (d, d, t, 4H, substituted phenyl), 3.71 (s, 2H, $O-CH_2-$), −2,73 (s, br, 2H, imino). $H_2P-CONH_2$: 8.82 (m, 8H, β-pyrrole), 8.09 (m, 6H, ortho phenyl), 7.79 (m, 9H, meta and para phenyl), 8.38−6.72 (d, d, t, 4H, substituted phenyl), 3.08 (s, 2H, $O-CH_2-$), 3.82 (s, br, 1H, N−H), 2.76 (s, br, 1H, N−H), −2.81 (s, br, 2H, imino). ZnP−COOH: 8.77 (m, 8H, β-pyrrole), 8.10 (m, 6H, ortho phenyl), 7.71 (m, 9H, meta and para phenyl), 7.46−6.96 (d, d, t, 4H, substituted phenyl), 4.05 (s, br, 2H, $O-CH_2-$); ESI mass in CH_2Cl_2, calcd. 752.2, found 751.6. $ZnP-CONH_2$: 8.78 (m, 8H, β-pyrrole), 8.16 (m, 6H, ortho phenyl), 7.71 (m, 9H, meta and para phenyl), 8.01−6.83 (d, d, s, 4H, substituted phenyl), 3.08 (s, 2H, $O-CH_2-$), 3.82 (s, br, 1H, N−H), 2.76 (s, br, 1H, N−H); ESI mass in CH_2Cl_2 cacld. 751.2, found 750.1.

Instrumentation. The UV−visible spectral measurements were carried out with a Shimadzu model 1600 UV-visible spectrophotometer. The fluorescence emission was monitored by using a Spex Fluorolog-tau spectrometer. A right angle detection method was used. The ^{1}H NMR studies were carried out on a Varian 400 MHz spectrometer. Tetramethylsilane (TMS) was used as an internal standard. Cyclic voltammograms were recorded on a EG&G model 263A potentiostat using a three electrode system. A platinum button or glassy carbon electrode was used as the working electrode. A platinum wire served as the counter electrode and a Ag wire (Ag/Ag^+) was used as the reference electrode. Ferrocene/ferrocenium redox couple was used as an internal standard. All of the solutions were purged prior to electrochemical and spectral measurements using argon gas. The computational calculations were performed by ab initio B3LYP/3-21G(*) methods with Gaussian 98[13] software package on various PCs and a SGI ORIGIN 2000 computer. The graphics of HOMO and LUMO coefficients were generated with the help of Gauss View software. The ESI mass spectral analyses of the newly synthesized compounds were performed by using a Fennigan LCQ-Deca mass spectrometer. For this, the compounds (about 0.1 mM concentration) were prepared in CH_2Cl_2, freshly distilled over calcium hydride.

Time-Resolved Emission and Transient Absorption Measurements. The picosecond time-resolved fluorescence spectra were measured using an argon ion pumped Ti:sapphire laser (Tsunami) and a streak scope (Hamamatsu Photonics). The details of the experimental setup are described elsewhere.[14] Nanosecond transient absorption spectra in the near-infrared region were measured by means of laser flash photolysis; 532 nm light from a Nd:YAG laser was used as the exciting source and a Ge avalanche photodiode module was used for detecting the monitoring light from a pulsed Xe lamp as described in our previous report.[14]

Results and Discussion

The "two-point" binding in the studied dimethylaminophenyl−zinc porphyrin−fullerene supramolecular assemblies was established from ^{1}H NMR and UV−visible absorption spectral, and ab initio computational modeling studies. Addition of either **1** or 2-(4′-pyridyl)fulleropyrrolidine, C_{60}py, to a solution of any of the donor porphyrins resulted in spectral changes characteristic of axially coordinated species, that is, the spectra exhibited red-shifted Soret and visible absorption bands with the appearance of isosbestic points[15] (Figure 2). Job's plots of method of continuous variation confirmed 1:1 complex formation. The formation constants, *K*, for the porphyrin−fullerene conjugates, determined from the UV−visible spectral data and by Scatchard plots[16] (Figure 2 inset), are found to be an order of magnitude higher for the two-point bound complexes compared to the one-point bound complex (Table 1). The higher values of *K* indicate stable complex formation as compared to the complexes formed by the "one-point" axial coordination.

The ^{1}H NMR spectral studies were performed to establish the occurrence of "two-point" binding in the studied supramolecular complexes. Figure 3 illustrates the spectrum of starting compounds, $ZnP-NH_2$ and 2-(4′-pyridyl)fulleropyrrolidine, and the supramolecular complex formed between these two entities. 2-(4′-Pyridyl)fulleropyrrolidine was utilized over **1** for ^{1}H NMR studies for its simplicity; however, it should be noted that similar spectral trends were observed when **1** was used to complex the functionalized zinc porphyrins. In the self-assembled complex, formed by mixing stoichiometric amounts of the fullerene and porphyrin derivatives, shielding of both the pyridine and pyrrolidine ring protons was observed. That is, the pyridine

TABLE 1: Binding Constants (K), Fluorescence Lifetimes (τ_f),[a] Charge-Separation Rate Constants ($k_{cs}^{singlet}$), Charge-Separation Quantum Yields ($\Phi_{cs}^{singlet}$), and Charge-Recombination Rate Constants (k_{cr}) for *N*,*N*-Dimethylaminophenyl−Zinc Porphyrin−C_{60} Triads in *o*-Dichlorobenzene

complex	K, M^{-1}	τ_f[a]	$k_{cs}^{singlet}$, s^{-1} [b]	$\Phi_{cs}^{singlet}$ [b]	k_{cr}, s^{-1}	k_{cs}/k_{cr}
C_{60}py:ZnP	0.77×10^4	1.85 ns (100%)	6.3×10^7	0.12	3.0×10^7	2
1:ZnP	0.78×10^4	71 ps (27%) 2.03 ns (73%)	1.5×10^8 [c]	0.22[c]	3.4×10^7	4
1:ZnP−$CONH_2$	3.1×10^4	69 ps (81%) 1.6 ns (19%)	1.8×10^9 [c]	0.77[c]	3.1×10^7	58
1:ZnP−COOH	10×10^4	8 ps (75%) 2.28 ns (25%)	1.0×10^9 [c]	0.67[c]	2.3×10^7	43

[a] The singlet lifetimes of ZnP, ZnP−$CONH_2$, and ZnP−COOH in deareated *o*-dichlorobenzene were found to be 1.92, 1.97, and 2.35 ns (monoexponential decay), respectively. [b] $k_{cs}^{singlet} = (1/\tau_f)_{sample} - (1/\tau_f)_{ref}$; $\Phi_{cs}^{singlet} = [(1/\tau_f)_{sample} - (1/\tau_f)_{ref}]/(1/\tau_f)_{sample}$. [c] Values are average ones.

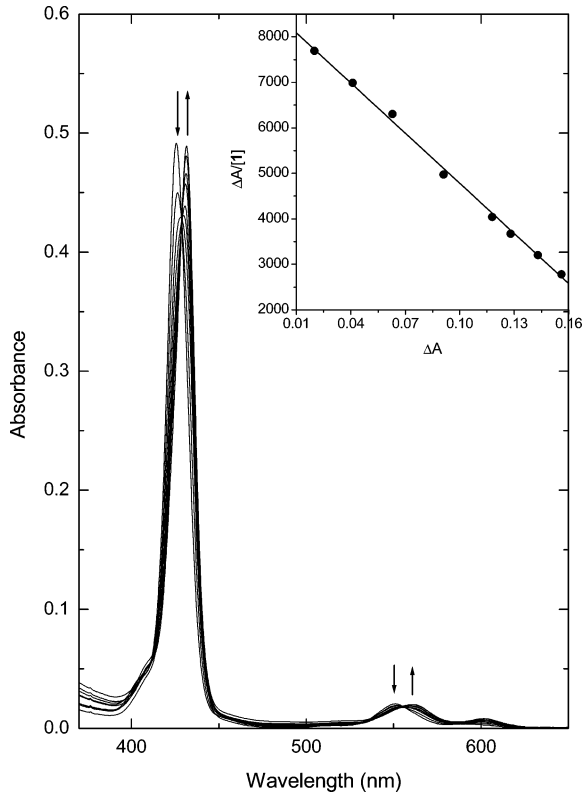

Figure 2. UV-visible spectral changes observed for ZnP−$CONH_2$ (2 μM) on increasing addition of **1** (2.6−68.5 μM) in *o*-dichlorobenzene.

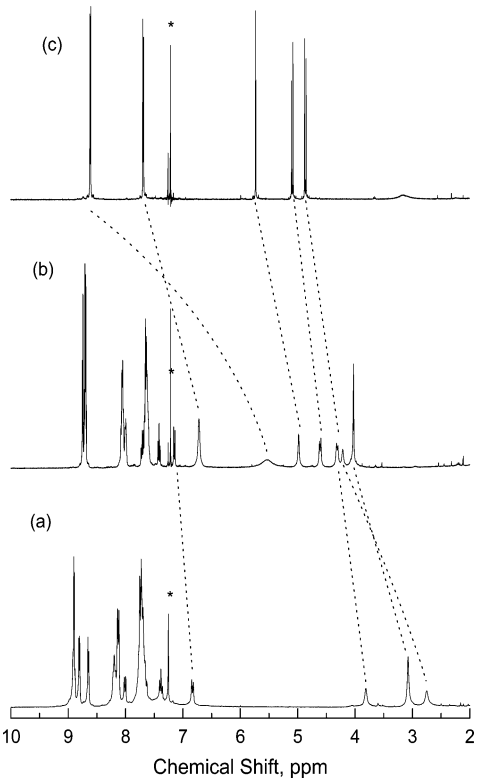

Figure 3. ^{1}H NMR spectrum of (a) ZnP−$CONH_2$ (15 mM), (b) ZnP−$CONH_2$:2-(4′-pyridyl)fulleropyrrolidine dyad (15 mM), and (c) 2-(4′-pyridyl)fulleropyrrolidine (15 mM) in $CDCl_3/CS_2$ (1:1 v/v). The asterisk (∗) indicates solvent impurity.

peaks of 2-(4′-pyridyl)fulleropyrrolidine located at 8.60 and 7.40 ppm were shifted to 5.52 and 6.70 ppm upon complexation, while the pyrrolidine peaks located at 5.72, 5.08, and 4.86 ppm were shifted to 4.98, 4.59, and 4.29 ppm, respectively. The greater shift observed for the pyridine protons can be rationalized by the greater porphyrin ring currents experienced by the axially coordinated pyridine ring.[7g] Interestingly, an opposite trend in the spectral shifts for the peak corresponding to the zinc porphyrin pendant arm was observed. The −O−CH_2−$CONH_2$ peaks located at 3.82, 3.07, and 2.72 ppm appeared at 4.20 and 4.02 ppm in the supramolecular complex. The substituted phenyl ring protons of the zinc porphyrin also revealed a deshielding of about 0.3 ppm in the supramolecular complex. These results along with the higher binding constants clearly demonstrate the two modes of binding in the supramolecular complex.

Ab Initio B3LYP/3-21G(*) Modeling of the Supramolecular Triad. To gain insights into the geometry and electronic structure of the self-assembled triads, computational studies have been performed by using density functional methods (DFT) at the B3LYP/3-21G(*) level. The DFT methods over the Hartree−Fock or semiempirical approach are chosen because recent studies have shown that the DFT methods at the 3-21G(*) level predict the geometry and electronic structure accurately for covalently linked ferrocene−fullerene−nitroaromatic entities bearing dyad and triads[17a−c] and also for self-assembled via base-pairing fullerene−uracil·adenine conjugates.[17d] In our calculations, first, both **1** and the zinc porphyrins were fully optimized to a stationary point on the Born−Oppenheimer potential energy surface and then allowed to interact. Figure 4a presents the optimized structure of the **1**:ZnP−COOH triad, while for the **1**:ZnP−$CONH_2$ triad, the structure is given in the Supporting Information (SI). In the optimized structures, the zinc−pyridine nitrogen distance was found to be 2.01 Å, close to that obtained earlier for the C_{60}Py:ZnP complex by X-ray crystallography.[7d]

The interatomic distances for the hydrogen-bonding functionalities for both **1**:ZnP−COOH and **1**:ZnP−$CONH_2$ are shown in Scheme 1a. The distance between the pyrrolidine ring nitrogen and the carbonyl oxygen of the pendant acid group was found to be 2.85 Å for **1**:ZnP−COOH, while this distance for **1**:ZnP−$CONH_2$ was equal to 2.87 Å. The distance between the pyrrolidine ring nitrogen and the carboxylic acid hydrogen was found to be 1.57 Å for **1**:ZnP−COOH, while the similar distance resulting from the amide hydrogen to the pyrrolidine

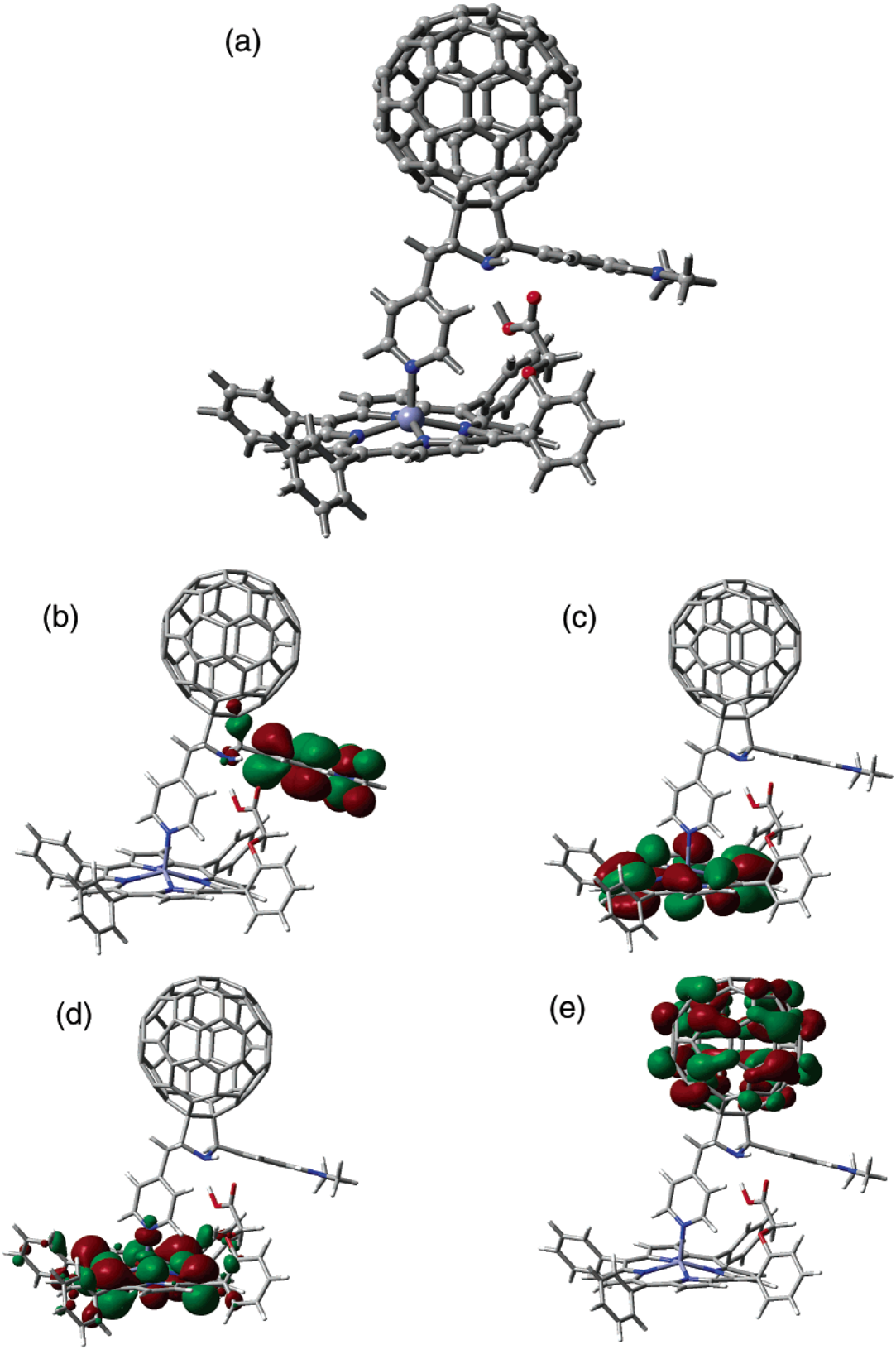

Figure 4. Ab initio B3LYP/3-21G(*) calculated (a) optimized structure, (b) HOMO-2, (c) HOMO-1, (d) HOMO, and (e) LUMO for the self-assembled **1**:ZnP−COOH triad.

ring nitrogen was found to be 2.06 Å. Two model self-assembled complexes, pyrrolidine:acetic acid and pyrrolidine:acetamide, were also investigated. As depicted in Scheme 1b, the optimized structure of these complexes revealed structures similar to that shown in Scheme 1a with slightly shorter interatomic distances. The slightly longer distances in **1**:ZnP−COOH and **1**:ZnP−$CONH_2$ could be due to steric strain or the electronic/geometric effects on the pyrrolidine nitrogen caused by the fullerene spheroid.[17a] These results suggest the existence of hydrogen-bonding interactions in addition to the axial Zn−N coordination in the self-assembled triads. For **1**:ZnP−COOH, the center-to-center distance, that is, the distance between the zinc and the

SCHEME 1: Ab Initio B3LYP/3-21G(*) Optimized Bond Distances for the Hydrogen-Bonding Site of 1:ZnP−COOH and 1:ZnP−$CONH_2$ and Model Compounds

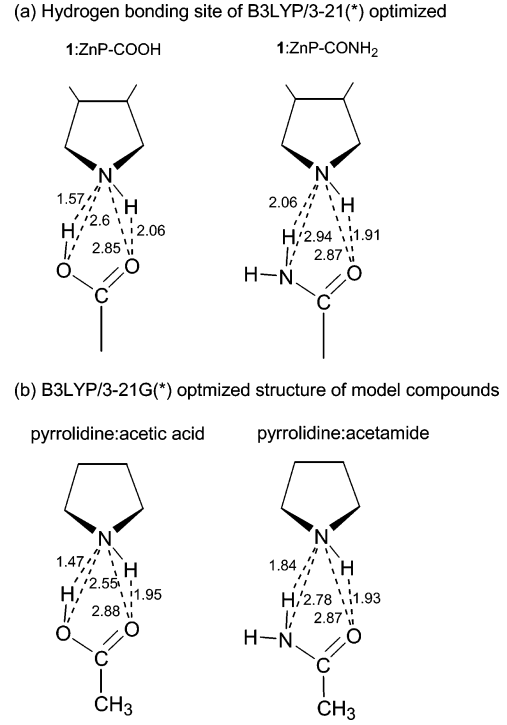

center of fullerene spheroid was evaluated to be 12.96 Å while the distance between the center of porphyrin and the N of dimethylaminophenyl was 11.64 Å. Similarly, for **1**:ZnP−$CONH_2$, these distances were found to be 12.36 and 11.54 Å, respectively. These results, along with the higher binding constant values and ^{1}H NMR results, suggest that employing multiple modes of binding yields more stable complexes with defined distance and orientation.

The frontier HOMO-2, HOMO-1, HOMO, and LUMO orbitals of the **1**:ZnP−COOH triad are shown in Figure 4b−e, while the frontier orbitals for the **1**:ZnP−$CONH_2$ triad are given in the SI. The HOMO and HOMO-1 were found to be localized on the zinc porphyrin π-system, while the majority of the HOMO-2 was found to be on the dimethylaminophenyl group of **1**. It is remarkable that the orbital energy sequence using the B3LYP/3-21G(*) level of ab initio DFT theory is able to reproduce or predict the sequence of the redox potentials observed (vide infra) for systems of this size with closely spaced oxidation potentials. A small amount of the HOMO was found on the axially ligated pyridine entity, while a small portion of the HOMO-2 was also found on the pyrrolidine ring of **1**. The LUMO, LUMO+1, and LUMO+2 were found to be on the C_{60} entity of **1**. As discussed in the next paragraph, the HOMO and LUMO track the site of electron transfer of the different redox entities of the triad.

Cyclic voltammetric (CV) studies were performed to evaluate the potentials of the different redox entities utilized to form the supramolecular triads. The cyclic voltammogram of zinc tetraphenylporphyrin, ZnP, is shown in Figure 5a. The redox potentials corresponding to the oxidation were located at 0.28 and 0.62 V vs Fc/Fc^+, while the potentials corresponding to the reduction were located at −1.92 and −2.23 V vs Fc/Fc^+ respectively. These potentials are not much different from the other zinc porphyrins employed in the present study indicating little or no electronic interactions between the porphyrin π-systems and the pendant amide or carboxylic acid groups.

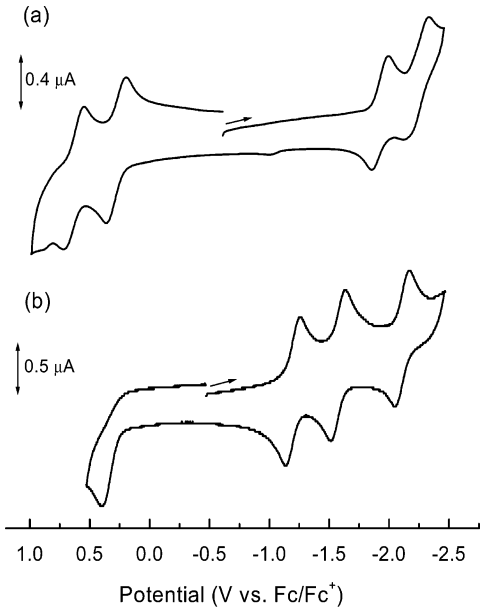

Figure 5. Cyclic voltammograms of (a) ZnP and (b) **1** in *o*-dichlorobenzene containing 0.1 M $(TBA)ClO_4$. Scan rate = 100 mV/s.

The CV of **1** revealed peaks corresponding to the oxidation of the *N*,*N*-dimethylaminophenyl entity in addition to the C_{60} entity. The oxidation process of the *N*,*N*-dimethylaminophenyl entity was found to be irreversible with the peak potential located at E_{pa} = 0.40 V vs Fc/Fc^+. Three one-electron reversible waves located at $E_{1/2}$ = −1.17, −1.55, and −2.07 V vs Fc/Fc^+ were also observed for **1** within the potential window of the solvent corresponding to the reductions of the C_{60} entity (Figure 5b). The magnitude of the potentials of the different redox entities, that is, the sequence of the site of electron-transfer, tracks the orbital energies predicted by the B3LYP/3-21(*) results. The C_{60} reduction potentials of **1** were found to be almost similar to that reported earlier for fulleropyrrolidine derivatives[7g,17,18] indicating little or no electronic interactions between the C_{60} and *N*,*N*-dimethylaminophenyl entities. The close spacing between the first oxidation of zinc porphyrin and the dimethylaminophenyl entities suggests the possibility of the occurrence of a hole migration or hole exchange between $ZnP^{+\bullet}$ and the dimethylaminophenyl entity formed during the photoinduced electron-transfer process in the supramolecular triads.

Photochemical Studies. The photochemical behavior of the "two-point" bound supramolecular triads was investigated, first, by using steady-state fluorescence measurements. On addition of either compound **1** or 2-(4′-pyridyl)fulleropyrrolidine to an argon-saturated *o*-dichlorobenzene solution of zinc porphyrins, ZnP−COOH or ZnP−NH_2, they exhibited a fluorescence intensity decrease until about 30%. Scanning the emission wavelength to longer wavelength regions (700−800 nm) revealed a weak emission band at 710 nm corresponding to the emission of the C_{60} moiety (data not shown). The intensity of this band for a given concentration of fulleropyrrolidine was found to be almost the same as that obtained in the absence of added zinc porphyrins. Changing the excitation wavelength from 554 to 410 nm also revealed similar observations with slightly enhanced emission of the fullerene entity due to its higher absorbance at 410 nm. These results suggest that energy transfer from the singlet excited zinc porphyrin to fulleropyrrolidine is not necessarily to be considered as a cause of the fluorescence quenching. Interestingly, the present steady-state fluorescence studies revealed efficient quenching of zinc porphyrin emission upon coordinating **1** and such quenching was found to be much

SCHEME 2: Proposed Mechanism of the Photochemical Charge Stabilization in the Self-Assembled 1:ZnP−COOH Triad

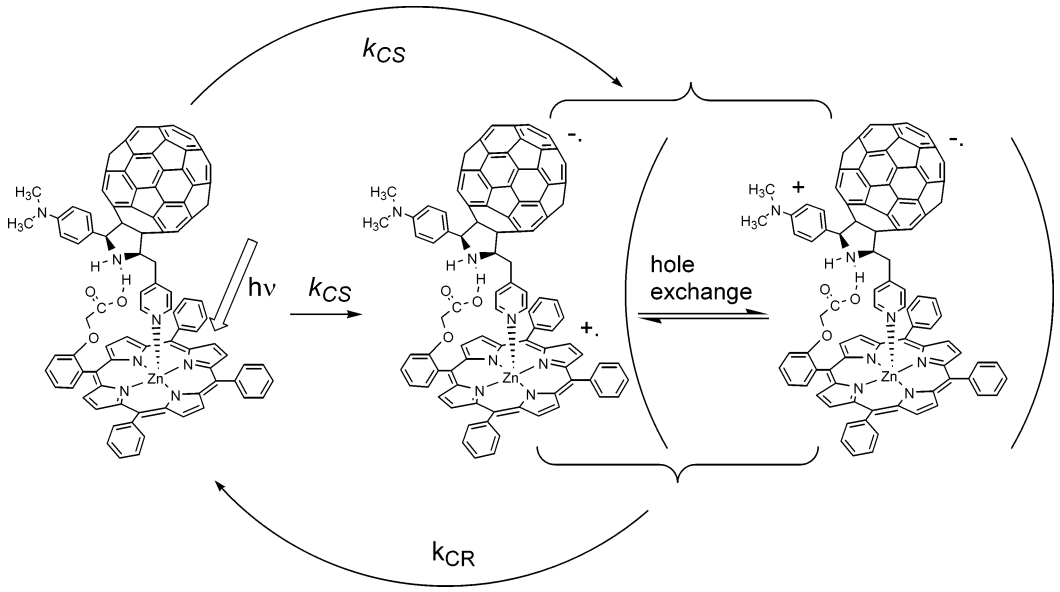

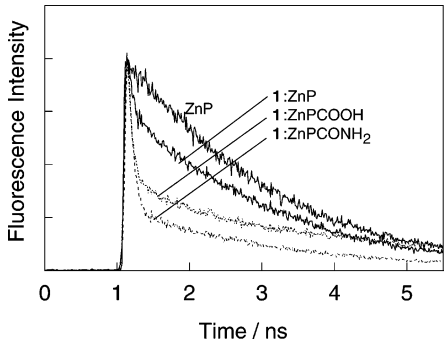

Figure 6. Fluorescence decay profiles of ZnP (0.1 mM) and **1**:ZnP's (0.1 mM:0.1 mM) in *o*-dichlorobenzene: $\lambda_{ex} = 410$ nm and $\lambda_{em} = 600$ nm.

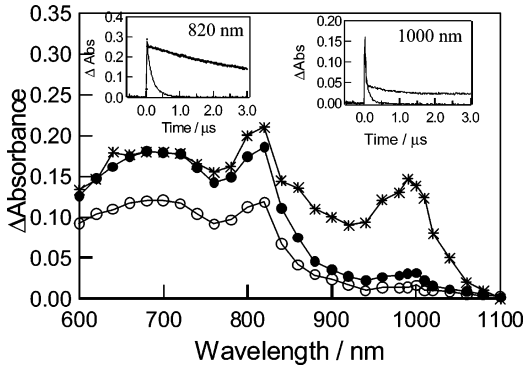

Figure 7. Transient absorption spectra obtained by 532 nm laser light of **1**:ZnP−$CONH_2$ (0.1 mM, 1:1 equiv) in *o*-dichlorobenzene: (∗) 0.01 μs; (●) 0.25 μs; (○) 2.5 μs. Inset shows time profiles of the 820 and 1000 nm bands.

more for the two-point bound complexes than the one-point bound complex. That is, the amount of **1** needed to quench the porphyrin fluorescence was ∼25% less for the two-point bound complexes than that needed for the one-point bound complex.

Time-profiles of the emission of the singlet excited state of zinc porphyrins are shown in Figure 6. The zinc porphyrins, ZnP, ZnP−$CONH_2$, and ZnP−COOH, in deareated *o*-dichlorobenzene revealed monoexponential decay with lifetimes of 1.92, 1.97, and 2.35 ns, respectively. Upon self-assembly of **1** with zinc porphyrins, quick fluorescence decay corresponding to the charge separation was observed. Such quick fluorescence decay was found to be much more efficient for the two-point bound complexes than the one-point bound complex indicating efficient charge separation for the two-point complexes. Clear shortening of the fluorescence lifetimes was not observed for a dyad formed by coordinating C_{60}py (bearing no dimethylaminophenyl entity) to ZnP indicating that the second electron donor, *N*,*N*-dimethylaminophenyl, is essential to accelerate the charge separation with average quantum yield more than 0.67. By assuming that the short lifetimes are due to the electron transfer within the supramolecular triads, we evaluated the charge-separated rates ($k_{cs}^{singlet}$) and quantum yield ($\Phi_{cs}^{singlet}$) in a usual manner employed in the intramolecular electron-transfer process.[19] Higher values of both $k_{cs}^{singlet}$ and $\Phi_{cs}^{singlet}$ were obtained for the supramolecular triads (Table 1).

The charge recombination processes were monitored by nanosecond transient absorption studies. Figure 7 shows a representative spectrum for the triad formed by self-assembly of **1** and zinc porphyrin appended with an amide group (ZnP−$CONH_2$). The spectrum recorded at 0.01 μs showed the radical anion of the C_{60} moiety around 1000 nm. The absorption bands at 700 and 870 nm correspond, respectively, to the triplet C_{60} and triplet ZnP−$CONH_2$.[7g] The absorption band of ZnP−$CONH_2^{+\bullet}$, expected to appear around 625 nm, was masked by the strong absorption bands of the triplet states of the C_{60} and ZnP moieties in this wavelength region. Interestingly, the spectrum recorded at the 0.25 μs time interval still revealed the existence of the 1000 nm band indicating the survival of the ion pair at longer time scales. The time profile monitored for the 1000 nm band revealed a two-step decay process, a quick decay process ($\tau_{1/2} = 30$ ns, $k = 3.1 \times 10^7$ s^{-1}) and a slow decay process of longer time scales ($\tau_{1/2} = 2000$ ns. $k = 3.5 \times 10^5$ s^{-1}). The quick decay process corresponds to the charge recombination (k_{cr}). The decay rates of the absorption bands of the triplet states (k_T) were found to be further slowed for this triad ($k_T = 1.1 \times 10^5$ s^{-1} at 600 nm and $k_T = 2.0 \times 10^5$ s^{-1} at 820 nm). Thus, it is suggested that in the slower decay part of 1000 nm time profile, a second slow charge separation process may be hidden, although it was difficult to separate it from that of the triplet-state absorption bands. Addition of dioxygen quenched the slow decay almost completely; however, this observation does not always deny the second charge recombina-

tion process, because dioxygen quenches the radical ion pairs with longer lifetime with the triplet character, in addition to the triplet states themselves. An examination of the calculated k_{cs}/k_{cr} ratio, a measure of excellence in the photoinduced electron-transfer systems, in Table 1 clearly demonstrates charge stabilization in the triads, that is, the magnitude of k_{cs}/k_{cr} depends on the *K* values. Larger *K* values facilitate the charge-separation process and induce slow charge recombination.

The efficient and fast charge separation followed by relatively slow charge recombination observed in the triads formed by coordinating **1** with zinc porphyrins can be rationalized as follows. From the redox potential values of the different components of the investigated triads, it is possible that upon the initial electron transfer from the singlet excited states of zinc porphyrin to **1**, the dimethylaminophenyl moiety of **1** plays the role of the second donor because of its relatively low oxidation potential. A slow second-step charge recombination is anticipated in these triads because of the hole exchange between the ZnP and the dimethylaminophenyl group of **1** in the $ZnP^{+\bullet}$:$C_{60}^{-\bullet}$ ion pair. This hole exchange and the irreversible redox behavior of the dimethylaminophenyl group is ultimately expected to slow the charge recombination process (Scheme 2). Our attempts to separate the second charge-recombination process in the two-step decay at 1000 nm and to locate the dimethylaminophenyl radical cation, which is expected to appear in the 400−500 nm region, were unsuccessful because of its low ϵ value and the intense bands of the triplet ZnP and C_{60} in this wavelength region.

In summary, we have designed a novel approach of "two-point" binding to obtain stable self-assembled supramolecular triads composed of *N*,*N*-dimethylaminophenylfullerene−pyridine bound to zinc porphyrins. The second mode of binding was accomplished via hydrogen bonding between the pyrrolidine ring nitrogen of the fulleropyrrolidine and the pendant acid or amide group of the porphyrin. In the supramolecular triads, the second electron donor, *N*,*N*-dimethylaminophenyl, is shown to promote efficient charge separation upon excitation of the zinc porphyrin to yield the radical ion pairs. The radical ion pairs thus generated are shown to undergo slow charge recombination to yield relatively long-lived (30−40 ns) charge-separated states. A hole exchange between the $ZnP^{+\bullet}$ and dimethylaminophenyl entity upon initial light-induced charge separation and the irreversible redox behavior of the dimethylaminophenyl group were attributed to be responsible for slowing down the charge-recombination process. Further work in this direction is in progress in our laboratories.

Acknowledgment. The authors are thankful to the donors of the Petroleum Research Fund administered by the American Chemical Society, National Institutes of Health (to F.D.), Japan Ministry of Education, Science, Technology, Culture and Sports, and Mitsubishi Foundation (to O.I. and M.F.) for support of this work. The authors are also thankful to the High Performance Computing Center of the Wichita State University for lending SGI ORIGIN 2000 computer time.

Supporting Information Available: Ab initio B3LYP/3-21G(*) optimized structure and HOMO and LUMO orbitals for the **1**:ZnP−$CONH_2$ supramolecular triad. This material is available free of charge via the Internet at http://pubs.acs.org.

References and Notes

(1) (a) Diesenhofer, J.; Michel, H. *Angew. Chem., Int. Ed. Engl.* **1989**, *28*, 829. (b) Feher, G.; Allen, J. P.; Okamura, M. Y.; Rees, D. C. *Nature* **1989**, *339*, 111. (c) McDermott, G.; Prince, S. M.; Freer, A. A.; Hawthornethwaite-Lawles, A. M.; Papiz, M. Z.; Cogdell, R. J.; Isaacs, N. W. *Nature* **1995**, *374*, 517.

(2) (a) Sutin, N. *Acc. Chem. Res*. **1982**, *15*, 275. (b) Wasielewski, M. R. *Chem. Rev*. **1992**, *92*, 435. (c) Gust, D.; Moore, T. A.; Moore, A. L. *Acc. Chem. Res*. **1993**, *26*, 198. (d) Paddon-Row, M. N. *Acc. Chem. Res*. **1994**, *27*, 18. (e) Hayashi, T.; Ogoshi, H. *Chem. Soc. Rev*. **1997**, *26*, 355. (f) Piotrowiak, P. *Chem. Soc. Rev*. **1999**, *28*, 143. (g) Guldi, D. M. *Chem. Soc. Rev*. **2002**, *31*, 22.

(3) (a) Kroto, H. W.; Heath, J. R.; O'Brien, S. C.; Curl, R. F.; Smalley, R. E. *Nature* **1985**, *318*, 162. (b) Kratschmer, W.; Lamb, L. D.; Fostiropoulos, F.; Huffman, D. R. *Nature* **1990**, *347*, 345.

(4) (a) Allemand, P. M.; Koch, A.; Wudl, F.; Rubin, Y.; Diederich, F.; Alvarez, M. M.; Anz, S. J.; Whetten, R. L. *J. Am. Chem. Soc*. **1991**, *113*, 1050. (b) Xie, Q.; Perez-Cordero, E.; Echegoyen, L. *J. Am. Chem. Soc*. **1992**, *114*, 3978.

(5) Imahori, H.; El-Khouly, M. E.; Fujitsuka, M.; Ito, O.; Sakata, Y.; Fukuzumi, S. *J. Phys. Chem. A* **2001**, *105*, 325.

(6) *Fullerene and Related Structures*; Hirsch, A., Ed.; Springer: Berlin, 1999; Vol. 199.

(7) (a) D'Souza, F.; Deviprasad, G. R.; Rahman, M. S.; Choi, J.-P. *Inorg. Chem*. **1999**, *38*, 2157. (b) Armaroli, N.; Diederich, F.; Echegoyen, L.; Habicher, T.; Flamigni, L.; Marconi, G.; Nierengarten, J.-F. *New J. Chem*. **1999**, 77. (c) Da Ros, T.; Prato, M.; Guldi, D. M.; Alessio, E.; Ruzzi, M.; Pasimeni, L. *Chem. Commun*. **1999**, 635. (d) D'Souza, F.; Rath, N. P.; Deviprasad, G. R.; Zandler, M. E. *Chem. Commun*. **2001**, 267. (e) Da Ros, T.; Prato, M.; Guldi, D. M.; Ruzzi, M.; Pasimeni, L. *Chem.—Eur. J*. **2001**, *7*, 816. (f) D'Souza, F.; Deviprasad, G. R.; El-Khouly, M. E.; Fujitsuka, M.; Ito, O. *J. Am. Chem. Soc*. **2001**, *123*, 5277. (g) D'Souza, F.; Deviprasad, G. R.; Zandler, M. E.; Hoang, V. T.; Arkady, K.; VanStipdonk, M.; Perera, A.; El-Khouly, M. E.; Fujitsuka, M.; Ito, O. *J. Phys. Chem. A* **2002**, *106*, 3243. (h) D'Souza, F.; Deviprasad, G. R.; Zandler, M. E.; El-Khouly, M. E.; Fujitsuka, M.; Ito, O. *J. Phys. Chem. B* **2002**, *106*, 4952. (i) Hauke, F.; Swartz, A.; Guldi, D. M.; Hirsh, A. *J. Mater. Chem*. **2002**, *12*, 2088. (j) Wilson, S. R.; MacMahon, S.; Tat, F. T.; Jarowski, P. D.; Schuster, D. I. *Chem. Commun*. **2003**, 226. (k) El-Khouly, M. E.; Rogers, L. M.; Zandler, M. E.; Gadde, S.; Fujitsuka, M.; Ito, O.; D'Souza, F. *ChemPhysChem* **2003**, *4*, 474. (l) El-Khouly, M. E.; Gadde. S.; Deviprasad, G. R.; Fujitsuka, M.; Ito, O. *J. Porphyrins Phthalocyanines* **2003**, *7*, 1.

(8) Meijer, M. D.; van Klink, G. P. M.; van Koten, G. *Coord. Chem. Rev*. **2002**, *230*, 141 and references therein.

(9) Maggini, M.; Scorrano, G.; Prato, M. *J. Am. Chem. Soc*. **1993**, *115*, 9798.

(10) (a) Deviprasad, G. R.; D'Souza, F. *Chem. Commun*. **2000**, 1915. (b) Smith, K. M. *Porphyrins and Metalloporphyrins*; Elsevier: New York, 1977.

(11) (a) *Org. Synth*. **1966**, *46*, 28. (b) *Org. Synth. Collect.* **1963**, *4*, 486.

(12) Dorough, G. D.; Miller, J. R.; Huennekens, F. M. *J. Am. Chem. Soc*. **1951**, *73*, 4315.

(13) Frisch, M. J.; Trucks, G. W.; Schlegel, H. B.; Scuseria, G. E.; Robb, M. A.; Cheeseman, J. R.; Zakrzewski, V. G.; Montgomery, J. A., Jr.; Stratmann, R. E.; Burant, J. C.; Dapprich, S.; Millam, J. M.; Daniels, A. D.; Kudin, K. N.; Strain, M. C.; Farkas, O.; Tomasi, J.; Barone, V.; Cossi, M.; Cammi, R.; Mennucci, B.; Pomelli, C.; Adamo, C.; Clifford, S.; Ochterski, J.; Petersson, G. A.; Ayala, P. Y.; Cui, Q.; Morokuma, K.; Malick, D. K.; Rabuck, A. D.; Raghavachari, K.; Foresman, J. B.; Cioslowski, J.; Ortiz, J. V.; Stefanov, B. B.; Liu, G.; Liashenko, A.; Piskorz, P.; Komaromi, I.; Gomperts, R.; Martin, R. L.; Fox, D. J.; Keith, T.; Al-Laham, M. A.; Peng, C. Y.; Nanayakkara, A.; Gonzalez, C.; Challacombe, M.; Gill, P. M. W.; Johnson, B. G.; Chen, W.; Wong, M. W.; Andres, J. L.; Head-Gordon, M.; Replogle, E. S.; Pople, J. A. *Gaussian 98*, revision A.7; Gaussian, Inc.: Pittsburgh, PA, 1998.

(14) (a) Matsumoto, K.; Fujitsuka, M.; Sato, T.; Onodera, S.; Ito, O. *J. Phys. Chem. B* **2000**, *104*, 11632. (b) Komamine, S.; Fujitsuka, M.; Ito, O.; Morikawa, K.; Miyata, T.; Ohno, T. *J. Phys. Chem. A* **2000**, *104*, 11497. (c) Yamazaki, M.; Araki, Y.; Fujitsuka, M.; Ito, O. *J. Phys. Chem. A* **2001**, *105*, 8615.

(15) (a) D'Souza, F.; Hsieh, Y.-Y.; Deviprasad, G. R. *Inorg. Chem*. **1996**, *35*, 5747. (b) Nappa, M.; Valentine, J. S. *J. Am. Chem. Soc*. **1978**, *100*, 5075.

(16) (a) Scatchard, G. *Ann. N. Y. Acad. Sci*. **1949**, *51*, 661. (b) *Quantitative Chemical Analysis*, 6th ed.; Harris, D. C., Ed.; W. H. Freeman and Company: New York, 2003; pp 439−440.

(17) (a) D'Souza, F.; Zandler, M. E.; Deviprasad, G. R.; Kutner, W. *J. Phys. Chem. A* **2000**, *104*, 6887. (b) D'Souza, F.; Zandler, M. E.; Smith, P. M.; Deviprasad, G. R.; Arkady, K.; Fujitsuka, M.; Ito, O. *J. Phys. Chem. A* **2002**, *106*, 649. (c) Zandler, M. E.; Smith, P. M.; Fujitsuka, M.; Ito, O.; D'Souza, F. *J. Org. Chem*. **2002**, *67*, 9122. (d) Marczak, R.; Hoang, V. T.; Noworyta, K.; Zandler, M. E.; Kutner, W.; D'Souza, F. *J. Mater. Chem*. **2002**, *12*, 2123.

(18) (a) Kutner, W.; Noworyta, K.; Deviprasad, G. R.; D'Souza, F. *J. Electrochem. Soc*. **2000**, *147*, 2647. (b) Deviprasad, G. R.; Rahman, M. S.; D'Souza, F. *Chem. Commun*. **1999**, 849.

(19) D'Souza, F.; Gadde, S.; Zandler, M. E.; Arkady, K.; El-Khouly, M. E.; Fujitsuka, M.; Ito, O. *J. Phys. Chem. A* **2002**, *106*, 12393.